

Surface Science Letters

Electron-stimulated surface reactions in ReO_3

R. Ai, H.-J. Fan and L.D. Marks

Center for Surface Radiation Damage Studies, Department of Materials Science & Engineering, Northwestern University, Evanston, IL 60208, USA

Received 6 November 1991; accepted for publication 1 May 1992

Effects of electron irradiation on ReO_3 supported on different substrates (carbon and silicon monoxide) in both non-UHV and UHV environments were investigated using high resolution electron microscopy. It was observed that clean ReO_3 was stable under electron irradiation in a carbon free environment. When carbon was present, electron irradiation induced surface reactions of ReO_3 with carbon to form a metastable ReC phase. ReC has a NaCl fcc structure and a lattice parameter of 4.00 ± 0.05 (Å). The kinetics of the reaction were found to be linear with time.

1. Introduction

Studies of electron-induced surface desorption and reaction are of both scientific and technological interest, and therefore have been the focus of many investigations in recent years. From the theoretical point of view, investigations of such processes provide insight into the nature of surface bonding [1]. The technological importance is in many areas. For example, a space shuttle in the space environment experiences electron irradiation with a wide range energy spectrum which stimulates surface desorption and reaction, resulting in materials degradation [2]. In the laboratory, electron irradiation is encountered in every instrument that uses electron beams as a probe. Another example is lithography using an intense electron beam.

Transition metal oxides (TMO) are particularly susceptible to electron radiation damage during electron microscopy [2–6]. The most commonly ascribed mechanism for the damage process in TMO involves the excitation of core levels followed by an intra Auger decay, and is generally known as the K–F mechanism [7]. While previous studies have been focused on oxides such as TiO_2 , V_2O_5 and WO_3 which are insula-

tors or semiconductors, very little is known about the effect of high energy electron irradiation on metallic oxides. Due to its marked metallic property, ReO_3 was chosen to extend the microscopy studies of DIET to metallic oxides.

In a conventional electron microscope, the vacuum is on the order of 10^{-7} Torr. This means that the solid surface in an electron microscope will be covered by a monolayer of hydrocarbon contaminants within a few seconds. In general the surface layer of hydrocarbon contaminants tends to decompose into carbon under electron irradiation. In this case, the system under study becomes C/ ReO_3 , analogous to gases adsorbed on the surface of a conducting solid, which have been studied intensely [8]. Surface desorption and reaction processes in these systems are related in many respects to gas phase dissociation. In gas phase dissociation, the electronic excitation is localized long enough that the electronic excitation can be converted into kinetic energy, leading to molecular dissociation [9]. In comparing the free molecule to the surface of a conducting solid, while the primary electronic excitation is very similar, the path for energy dissipation is different. The important changes are the presence of a conducting substrate which provides the

pathway for energy redistribution, so that the surface electronic excitations can be delocalized into the substrate. In fact, in these systems the probability of desorption depends strongly on the electronic coupling between the gas adsorbates and the substrates, and may vary by many orders of magnitudes [10–15].

Vast amounts of experimental evidence for surface dissociation and reactions of molecules on metals have been documented. For instance, Burns et al. [16] reported the dissociation of NO_2 on Pt(111) into NO and O with a threshold of 10–15 eV; So et al. [17] observed the dissociation of NO into N_2O on the Ag(111) surface; and the surface modification of $\text{p}(2 \times 2)\text{S}$ and $\text{p}(2 \times 2)\text{Se}$ on Pt(111) induced by CO was investigated by Kiskinova et al. [18].

In this Letter, the effects of electron irradiation on ReO_3 are reported, and the role of carbon on the surface investigated. A surface reaction of ReO_3 with carbon was observed.

2. Experiment

Samples of high purity ReO_3 powders (99.999%) supported on holey carbon or silicon monoxide (SiO) films were used. Each sample was baked on a 150 W light bulb to reduce surface hydrocarbon contaminations just prior to insertion into a Hitachi H-9000 electron microscope. For UHV observation, samples were annealed at about 600°C in 1 Torr partial pressure of high purity oxygen for about half hour before being loaded into the Hitachi UHV H-9000 electron microscope. The H-9000 has a vacuum of approximately 3×10^{-7} Torr and the UHV H-9000 has a stable operation pressure of 2×10^{-10} Torr. The electron flux was measured by an exposure meter which was calibrated by a Faraday cup. Microscope observations were made with both microscopes operated at 300 kV accelerating voltage. During observation, the electron flux was maintained at about 5.0 A/cm^2 . The structure of the new phase was identified using selected-area electron diffraction, optical diffraction, and high resolution imaging.

3. Results

3.1. Non-UHV on carbon substrates

The initial studies were carried out in the non-UHV environment of the Hitachi H-9000 electron microscope and generally on holey carbon substrates. Fig. 1 shows the selected area diffraction patterns taken from a ReO_3 crystal

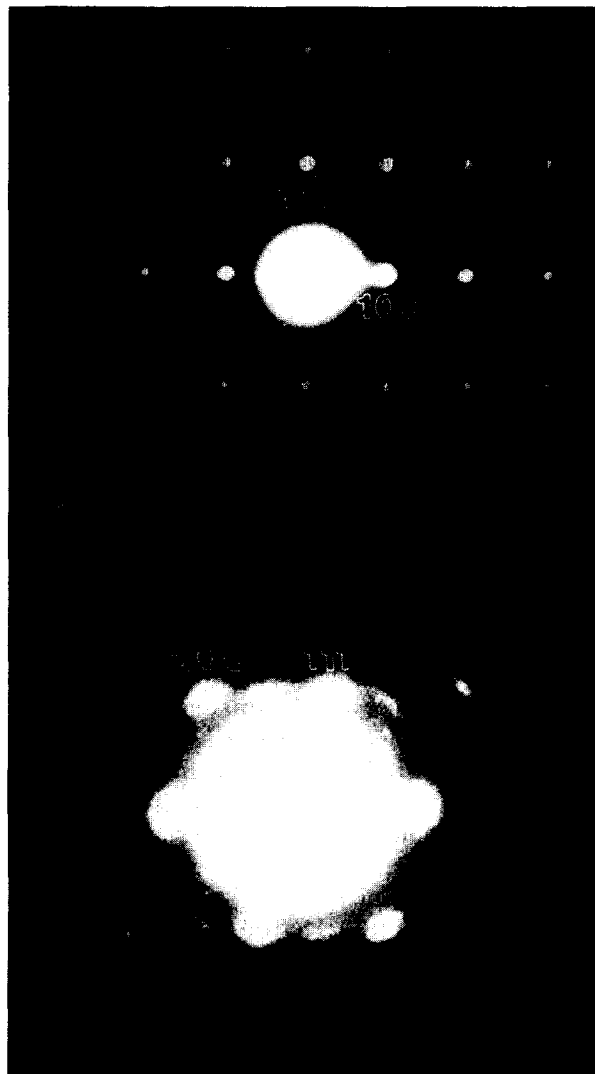


Fig. 1. Time sequence of selected area diffraction patterns taken along [011]: (a) initial; (b) after 30 min electron irradiation.

oriented along [011]. Fig. 1a was taken as soon as the crystal was tilted to the zone axis. Fig. 1b was taken after 30 min electron irradiation. In this diffraction pattern, a new set of diffraction spots appeared, indicating the formation of a new phase. The new phase can be indexed as a fcc

structure with an [011] orientation and a lattice parameter of 4.00 ± 0.05 (Å).

Fig. 2 shows a time sequence of high resolution images taken from the same crystal. Fig. 2a was taken as soon as the bulk crystal was tilted to the [011] zone axis (about 5 min), which shows

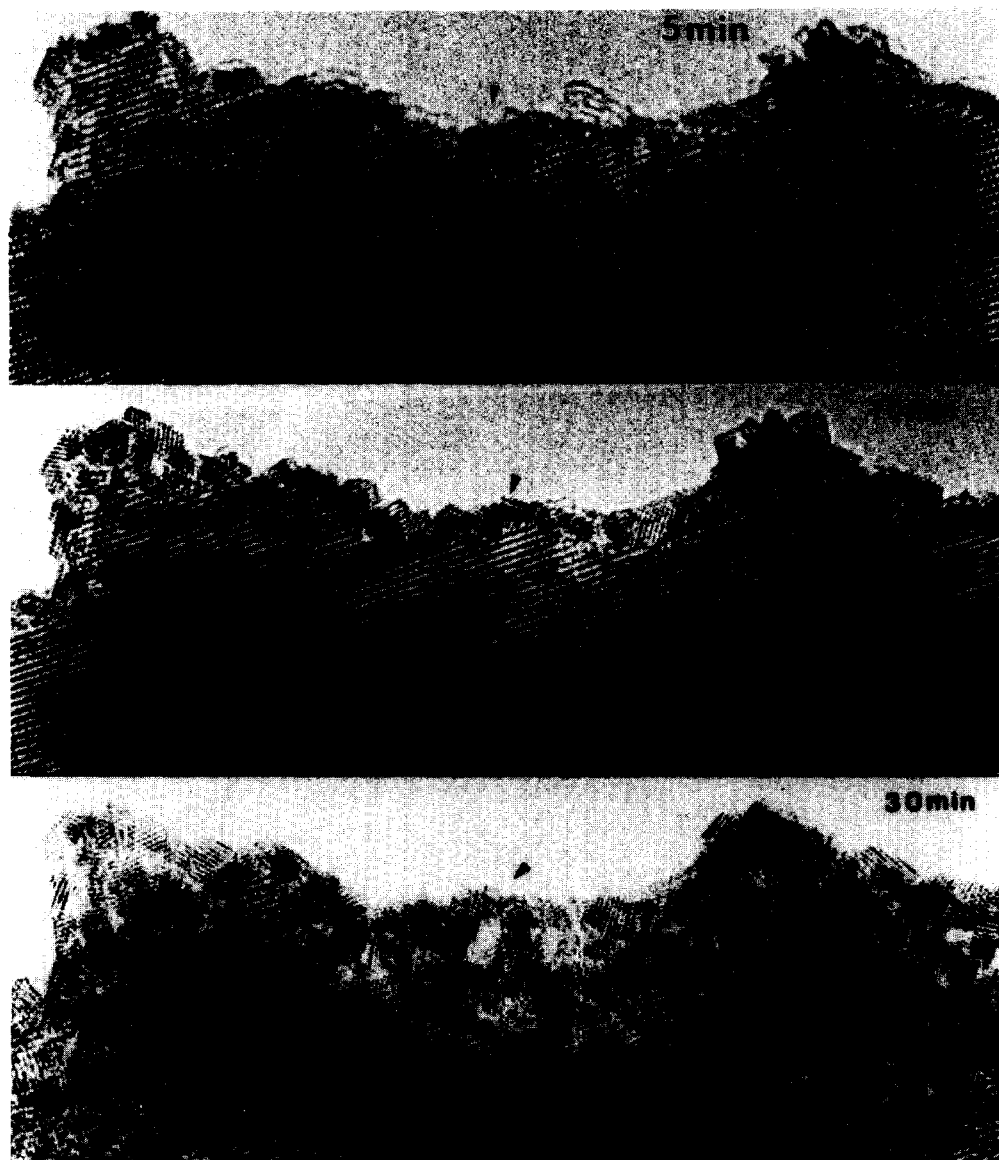


Fig. 2. Time sequence of high resolution images taken along [011]: (a) initial (5 min); (b) after 15 min; (c) after 30 min electron irradiation.

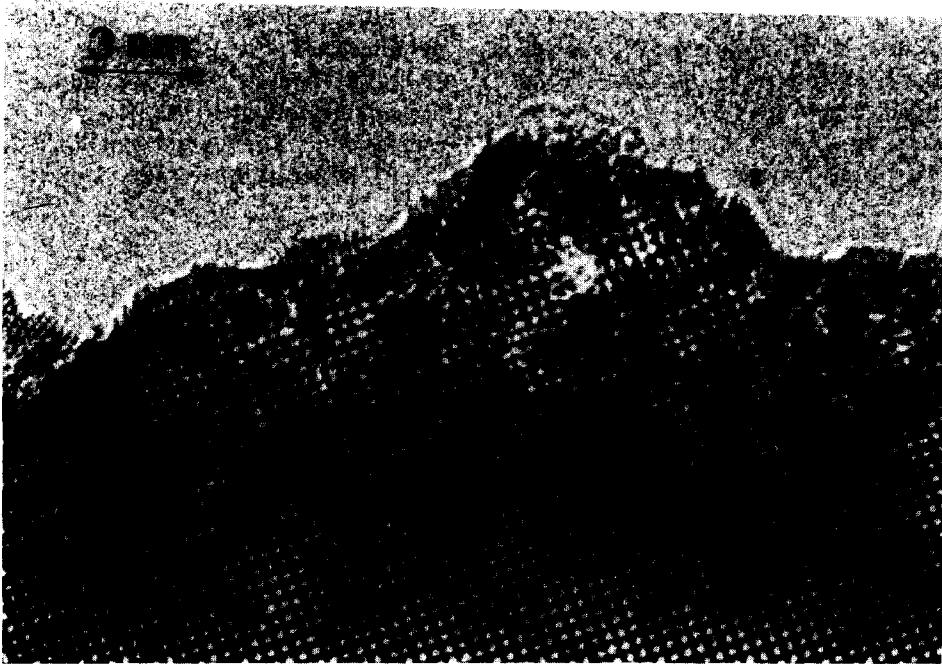


Fig. 3. High resolution image taken along [100] after about 20 min electron irradiation.



Fig. 4. High resolution image taken along [112] after about 20 min electron irradiation.

that a thin layer of the new phase has formed on the surface. With increasing irradiation time, this layer of new phase grew thicker as shown in fig.

2b. More importantly, fig. 2c which was taken after 30 min of irradiation, shows that the new phase not only formed on the surface that is

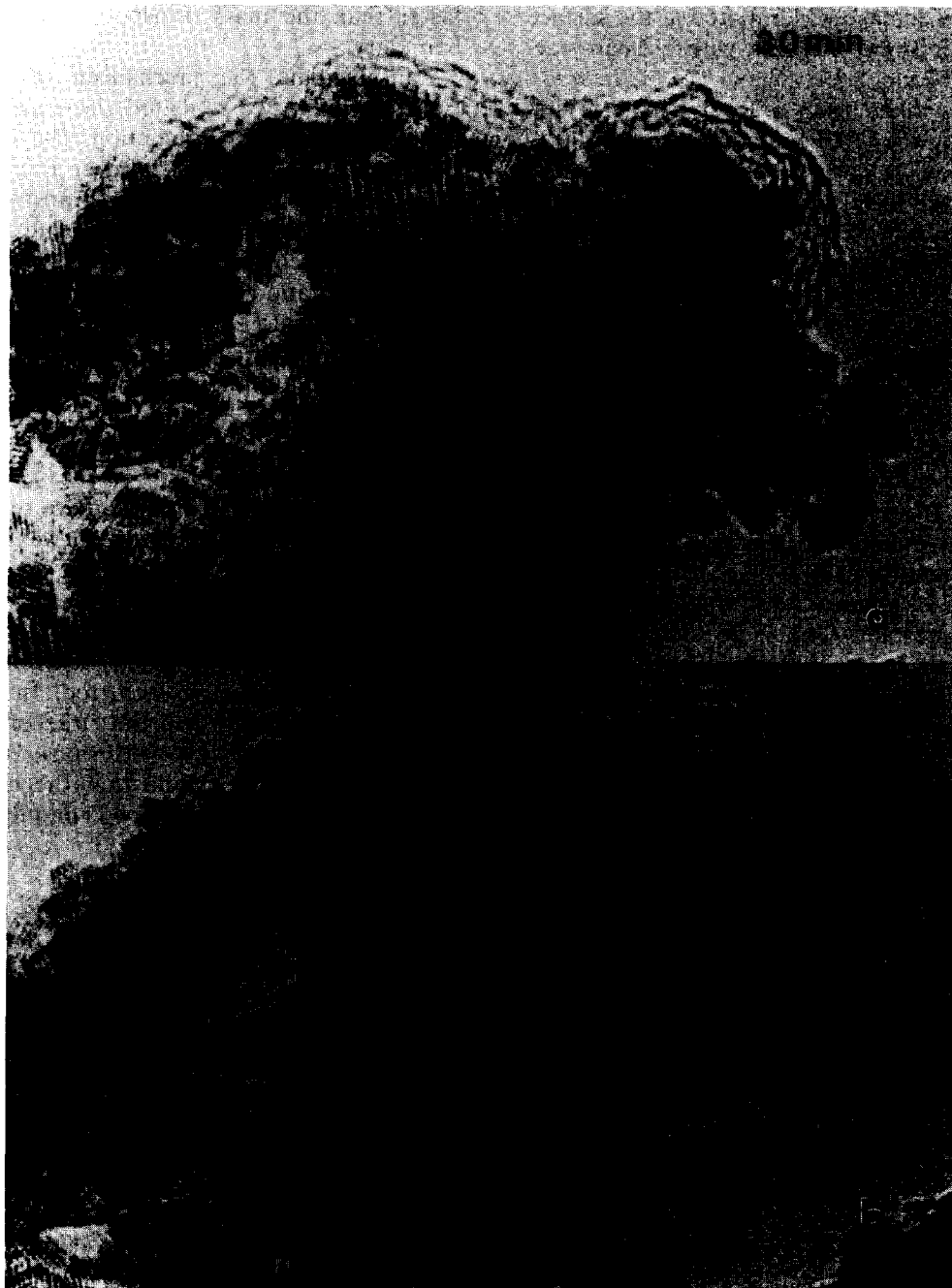


Fig. 5. High resolution images along [011] showing the decrease of a ReO₃ grain with increasing irradiation time. (a) 30 min; (b) 45 min.

parallel to the beam direction, but also formed on the top and bottom surfaces as indicated by arrows. This is a feature that is different from the damage behavior in V_2O_5 and WO_3 , where electron radiation damage was initiated at the surface and propagated into the bulk with a clear reaction front [5,6].

Fig. 3 was taken from a ReO_3 single crystal oriented along the [100] zone axis after about 20 min irradiation. A layer of the same new phase can be observed in this image. The spacing of the lattice fringes indicated by arrows corresponds to the (111) planar distance of the new phase.

The same phase transformation was observed in a ReO_3 single crystal oriented along [112]. As shown in fig. 4, a thin layer of the new phase can be seen after about 20 min electron irradiation. However, it should be pointed out that the rates of the phase transformation along [100] and [112] are noticeably slower than the rate along [011]. Furthermore it was also observed that regardless of the crystal orientation, the new phase always has an orientation of [110].

In studies of phase transformations, two aspects are important. One is to study the final phase. The other is to study the kinetics, i.e., the rate of the phase transformation. The kinetics of the electron-induced phase transformation were measured by monitoring the decrease of the ReO_3 grain size with time and are shown in fig. 5. The

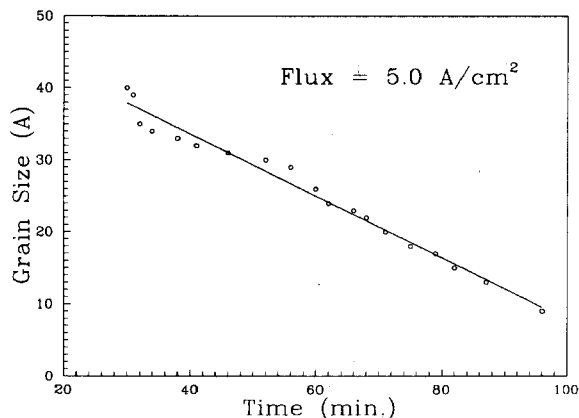


Fig. 6. A plot of the ReO_3 grain size as a function of time.

results shown in fig. 6 can be approximately fitted by a straight line, indicating that the kinetics of the reaction are interface-controlled. This type of reaction occurs when the reaction rate is much faster than the mass transport across the grain boundary.

To elucidate the mechanism of the phase transformation, we repeated the experiment using 100 keV electron irradiation. The same phase transformation occurred, however at a faster rate. This indicates that the phase transformation is not due to high energy processes, but low energy excitations such as plasmons. (Plasmon are the primary excitation mechanism for swift electrons, and they decay to electron-hole pairs. Of course, any low energy excitations, e.g. direct electron-hole pairs, will follow the same trend.)

3.2. Non-UHV on SiO substrates

More by accident than design, we repeated the experiment on a SiO substrate. It was found that during the observation, 50% of the time the same phase transformation took place, and the other 50% of the time it did not. Prior to minor maintenance of the instrument, no reaction was observed; after it reaction occurred. In a conventional microscope, there is too little control of the conditions to make any conclusions. However, it would be fair to conclude that the background gases were different in the two conditions.

3.3. UHV on carbon substrates

In a non-UHV environment, the clean time for surface observation is on the order of a few seconds for most materials. This means that as soon as samples are loaded into the microscope, the surface is contaminated. Under electron beam irradiation, these contaminants can interact with the final phase or the substrate leading to a misleading conclusion concerning the true effects of electron irradiation. Reactions due to interactions of the gaseous species in the vacuum with the irradiated sample can also occur. For example, for WO_3 , in a non-UHV environment the final phase observed is WO or WC, but in UHV, W metal is formed [19]. This illustrates the neces-

sity of performing experiments in a controlled environment.

We repeated the experiment in the UHV environment of the Hitachi UHV H-9000 electron microscope. Fig. 7 shows high resolution images taken along the [011] orientation, showing that the same phase transformation occurred, ruling out the possibility of interactions with the gaseous species in the vacuum. Note that this was with a carbon substrate.

3.4. UHV on SiO substrates

Samples on the SiO substrate were cleaned by annealing at about 600°C for about half hour in high purity oxygen with a partial pressure of 1

Torr in the side chamber of the instrument just before being loaded into the UHV microscope. The side chamber is directly vacuum coupled to the microscope. Samples after annealing had a clean surface as observed by high resolution images. Under these conditions, it was observed that electron beam irradiation had no effect on ReO_3 , indicating that clean ReO_3 crystals in a carbon free environment were stable under electron irradiation.

4. Discussions

A review of table 1 clearly indicates that clean ReO_3 is stable under electron irradiation, ne-

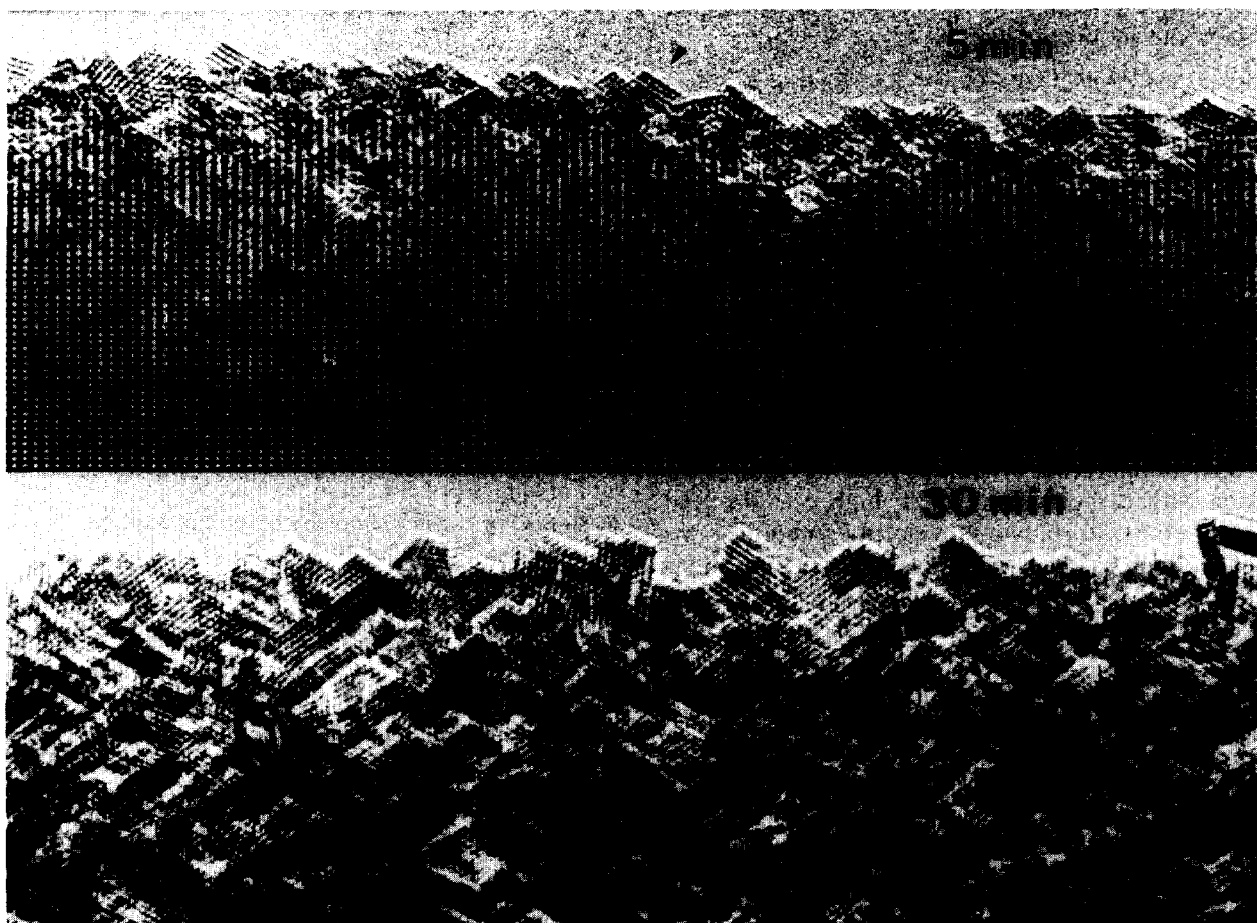


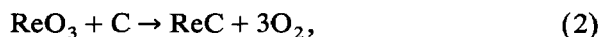
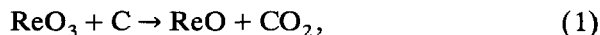
Fig. 7. Time sequence of high resolution images taken along [011] in UHV after: (a) 5 min; (b) 30 min electron irradiation.

Table 1
Summary of effects of electron irradiation on ReO_3

Substrate	Non-UHV	UHV
Carbon	New phase	New phase
Silica	50% New phase 50% No effect	No effect No effect

glecting slow knock-on damage. This is easy to understand in terms of the metallic properties of ReO_3 ; free electrons in the conduction band rapidly delocalized the electron excitation before it can be transferred into kinetic energy to cause atomic displacements. Whenever carbon is present, the electron beam will stimulate reactions of ReO_3 with carbon leading to a phase transformation; the electrons act as a catalyst in the reaction.

From the results, three possible reaction equations can be proposed:



The third one is unlikely since metal carbonates tend to decomposed into either carbides or monoxides under electron beam irradiation. It should be pointed out here that ReO has not been reported in the literature.

Rhenium is the only transition metal that does not form stable carbides. The Re-C phase diagram shows that at atmospheric pressure and room temperature, rhenium forms a solid solution with carbon. However at high pressure and high temperature, two polymorphic modifications of rhenium carbides were observed [20,21]. One is the hexagonal $\tau' = \text{MoC}$. The other is the cubic NaCl type. The lattice parameter of the cubic ReC is $4.005 \pm 0.002 \text{ \AA}$, corresponding to the lattice spacing of the new phase. Therefore the new phase can be identified as ReC , the high pressure, high temperature phase.

5. Conclusion

In conclusion, clean ReO_3 is stable to electron beam irradiation in a carbon free environment.

When carbon is present, the electron beam will stimulate reaction of ReO_3 with carbon to form ReC . ReC has a NaCl structure with a lattice parameter of $4.00 \pm 0.05 \text{ (\AA)}$. The reaction does not depend on the crystal orientation. However the reaction rate does. Along [011] the phase transformation has the fastest reaction rate and the kinetics of the reaction are interface controlled.

Acknowledgments

The authors would like to thank Dr. J.P. Zhang for many valuable discussions on the structural identification of the new phase. This work is supported by Air Force Office of Scientific Research on grant number of AFOSR 90-0045/B.

References

- [1] T.E. Madey, D.E. Ramaker and R. Stokbauer, *Ann. Rev. Phys. Chem.* 35 (1984) 215.
- [2] C.N. Fellas and S. Richardson, *IEEE Trans. on Nucl. Sci.* NS-28.6 (1981) 4523.
- [3] A.K. Petford, L.D. Marks and M. O'Keefe, *Surf. Sci.* 172 (1986) 496.
- [4] D.J. Smith, M.R. McCartney and L.A. Bursill, *Ultramicroscopy* 23 (1987) 299.
- [5] M.I. Buckett, J. Strane, D.E. Luzzi, J.P. Zhang, B.W. Wessel and L.D. Marks, *Ultramicroscopy* 29 (1989) 217.
- [6] H.J. Fan and L.D. Marks, *Ultramicroscopy* 31 (1989) 357.
- [7] M.L. Knotek and P.J. Feibelman, *Phys. Rev. Lett.* 40 (1978) 964.
- [8] See, articles in: *Desorption Induced by Electronic Transition, DIET III*, Eds. R.H. Stullen and M.L. Knotek (Springer, Berlin, 1988).
- [9] C. Lifshitz, *Adv. Mass Spectrosc.* 73 (1977) 3.
- [10] T.E. Madey and J.T. Yates, Jr., *J. Vac. Sci. Technol.* 8 (1971) 525.
- [11] D. Menzel, *Surf. Sci.* 47 (1975) 370.
- [12] M.L. Knotek, *Phys. Today* 37 (1984) 24.
- [13] See articles in *Desorption Induced by Electronic Transition, DIET I*, Eds. N.H. Tolk, M.M. Traum, J.C. Tully and T.E. Madey (Springer, Berlin, 1983).
- [14] See, articles in: *Desorption Induced by Electronic Transition, DIET II*, Eds. W. Brenig and D. Menzel (Springer, Berlin, 1985).
- [15] See, articles in: *Desorption Induced by Electronic Transition, DIET IV*, Eds. G. Betz and P. Varga (Springer, Berlin, 1990).

- [16] A.R. Burns, E.B. Stechel and D.R. Jennison, *Phys. Rev. B* 40 (1989) 9485.
- [17] S.K. So, R. Franchy and W. Ho, *J. Chem. Phys.* 91 (1989) 5701.
- [18] M. Kiskinova, A. Szabo and J.T. Yates, Jr., *Vacuum* 41 (1990) 82.
- [19] S.R. Singh and L.D. Marks, in preparation.
- [20] S.V. Popova and L.G. Boiko, *High Temp. High Pressures* 3 (1971) 237.
- [21] S.V. Popova, L.N. Formicheva and L.G. Khvostantsev, *JEPT Lett.* 16 (1972) 429.